Pichler, Thomas ; Renshaw, Carl E. ; Sültenfuß, Jürgen

Geogenic As and Mo groundwater contamination caused by an abundance of domestic supply wells

Journal Article as: peer-reviewed accepted version (Postprint)

DOI of this document*(secondary publication): https://doi.org/10.26092/elib/3183

Publication date of this document: 01/08/2024

* for better findability or for reliable citation

Recommended Citation (primary publication/Version of Record) incl. DOI:

Pichler, Thomas ; Renshaw, Carl E. ; Sültenfuß, Jürgen. 2017. Geogenic As and Mo groundwater contamination caused by an abundance of domestic supply wells. In: Applied Geochemistry, vol. 77, pp. 68-79. © Elsevier. DOI: 10.1016/j.apgeochem.2016.03.002.

Geogenic As and Mo groundwater contamination caused by an abundance of domestic supply wells

Thomas Pichler [a, *], Carl E. Renshaw [b], Jürgen Sültenfuß [c]

[a] *Institute of Geosciences, University of Bremen, 28359 Bremen, Germany*
[b] *Department of Earth Sciences, Dartmouth College, Hanover, NH 03755, USA*
[c] *Institute of Environmental Physics, University of Bremen, 28359 Bremen, Germany*

Keywords:
Molybdenum
Floridan Aquifer
Arsenic
Groundwater
Domestic supply wells

* Corresponding author.
E-mail address: pichler@uni-bremen.de (T. Pichler).

1. Introduction

The mobilization of naturally occurring (geogenic) arsenic (As) by exogenic perturbations to hydrogeological systems is well established. For example, Delemos et al. (2006) argue that leakage of organic contaminants from a landfill in New England, USA mobilized geogenic As by driving the microbially-induced reduction of As-bearing oxides. At other sites, pumping perturbed physiochemical conditions in the aquifer, mobilizing geogenic As. Harvey et al. (Harvey et al., 2002, 2006) argue that geogenic As at their field site in Bangladesh was mobilized as pumping for irrigation drew fresh organic carbon into the aquifer, which subsequently drove the microbially-induced reduction of As-bearing oxides. At other sites groundwater pumping has drawn oxygen-rich near surface water deeper into a nominally anoxic aquifer and resulted in the oxidation As-rich pyrite, releasing As into solution (e.g., Katz et al., 2009; Wallis et al., 2011).

Here we show that geogenic As can be similarly mobilized by endogenic hydrogeological perturbations, specifically the enhancement of the permeability of a confining layer by abundant domestic well drilling. This phenomenon is similar to, but more extensive than, the hydrologic short-circuiting provided by multi-aquifer wells, i.e., single wells penetrating and screened in multiple aquifers (Ayotte et al., 2011). As a result As concentrations of more than 30-times the US EPA enforced drinking water standard of 10 μg/L were measured in the groundwater beneath Lithia (Pichler and Sültenfuß, 2010). We further show that the groundwater mixing due to enhanced permeability also mobilizes geogenic molybdenum (Mo), resulting in groundwater Mo concentrations up to two orders of magnitude above the US EPA recommended value of 40 μg/L. This corresponds to Mo intakes nearly an order of magnitude greater than the tolerable upper intake level set by the Food and Nutrition Board of the U.S. National Academies Institute of Medicine (Food and Nutrition Board, 2001). Similar recent reports of high groundwater Mo concentrations in aquifers worldwide (e.g., Al Kuisi et al., 2015; Deverel and Millard, 1988; Johannesson et al., 2000; Leybourne and Cameron, 2008; Nicolli et al., 1989) have increased interest in understanding the factors causing the mobilization of Mo. Compared to As, however, the mobilization of geogenic Mo from the aquifer matrix is less studied, but similar to As, changes in redox conditions and water rock interaction seem to be the reason for elevated concentrations (e.g., Leybourne and Cameron, 2008). Toward this end, we applied hydrogeological modeling and chemical, stable isotope and radiogenic isotope tracers of groundwater flow pathways at a field site in the village of Lithia in central Florida (USA) to identify the cause of the high levels of As and Mo observed there. We specifically test if the As and Mo were mobilized by exogenic (i.e., extensive pumping from the well field located to the west of Lithia) or endogenic (i.e., drilling-induced enhancement of permeability) factors.

2. Study area

Following the discovery of more than 300 μg/L As in a newly installed municipal supply well near the village of Lithia in central Florida (Fig. 1(a)), 93 nearby private wells were sampled and analyzed by the Florida Department of Environmental Protection (DEP). Of those, 19 showed As concentrations above the current drinking water standard of 10 μg/L (Fig. 1(b)) and 34 wells had molybdenum (Mo) concentrations above 40 μg/L (Pichler and Sültenfuß, 2010). With no obvious anthropogenic or agricultural sources present, the As and Mo were likely of geogenic origin (Lazareva and Pichler, 2007; Pichler and Mozaffari, 2015; Pichler et al., 2011; Price and Pichler, 2006). Thus the high dissolved As and Mo concentrations in Lithia groundwater are likely the result of particular hydrogeological conditions which mobilized the As and Mo (Lazareva et al., 2015), but have not yet flushed dissolved As and Mo from these aquifers.

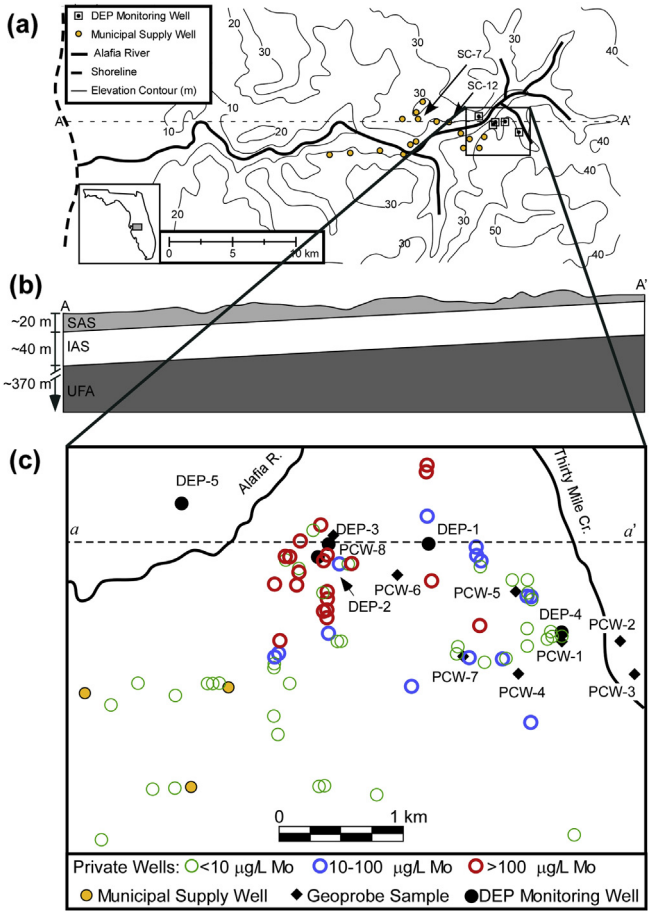

Fig. 1. (a) Topographic map of the study area showing locations of municipal supply wells and the Florida Department of Environmental Protection (FDEP) monitoring well clusters. (b) Simplified stratigraphic cross-section along line A–A′ showing three major hydro stratigraphic units in the study area. (c) Boxed region shows the locations of domestic supply wells (DSW), shallow monitoring wells (PCW) and FDEP monitoring well clusters (DEP). Molybdenum (Mo) concentrations are indicated for the DSW. A similar map with As concentrations can be found elsewhere (Pichler and Mozaffari, 2015). Dashed line shows location of transect a–a′ shown in detail in Fig. 7.

A multilayered aquifer system exists beneath Lithia, which can be subdivided into three distinct hydro stratigraphic units, which are, from the top down: the Surficial Aquifer System (SAS), the Intermediate Aquifer System (IAS), and the Upper Floridan Aquifer System (UFA). With exception of the uppermost sediments, calcium carbonates are the main lithology in all three hydro stratigraphic units, with occasional dolomite and clay minerals are present. Detailed mineralogical and lithological descriptions of these units and their regional hydrogeology in central Florida are described elsewhere (Hughes et al., 2009; Katz et al., 2007; Pichler and Mozaffari, 2015). Relevant hydrogeological characteristics of these units are briefly summarized here.

The unconfined SAS consists of unconsolidated to poorly indurated clastic deposits (Katz et al., 2009). Near the wells with high As and Mo concentrations the upper surface of the SAS is generally about 30 m above mean sea level (amsl) and ranges from about 65 m just to the east of the high-As wells to near zero where it intersects Hillsborough Bay about 35 km to the west. Near the high-As concentration wells, the base of the SAS is 10 m amsl and dips to the west at a slope circa 0.001. The SAS generally is not used as a

major source of water supply because of the relatively low yields to wells (less than 19 L/min), high Fe content, and the potential for contamination. Water table elevations in the SAS generally are above the potentiometric surface of the UFA, indicating downward groundwater flow from the SAS to the IAS and UFA (Katz et al., 2009).

The IAS consists of several water-bearing units separated by confining units, which are composed mainly of the siliciclastic Hawthorn Group with interlayered sequences of more and less permeable carbonates, sands and clays (Scott, 1988, 1990). Near the highest As concentrations, the bottom of the IAS is about −30 m amsl and dips to the west at a slope circa 0.001.

The UFA is the major source of water supply within the study area and consists of permeable limestone and dolomite deposited in a shallow marine environment (Green et al., 1995; Miller, 1986). Carbonate deposition was interrupted at first periodically, and finally completely, with the influx of the siliciclastic sediments eroded from the Appalachian Mountains that form the IAS. The Tampa Member of the Arcadia Formation belongs hydrostratigraphically to the UFA, although it is the lowermost stratigraphic unit of the Hawthorn Group (Miller, 1986). Within the region of high As concentrations, the bottom of the UFA is about −400 m amsl and dips to the west at a slope circa 0.001.

The median Mo and As concentrations in the IAS and UFA matrix are in the range between 2 and 3 mg/kg and vary significantly with depth (Pichler and Mozaffari, 2015). The distribution of values is heavily skewed due to occasionally high values of up to 100 mg/kg for As and up to 880 mg/kg for Mo. Arsenic and Mo concentrations are generally highest in the IAS and return to expected values for crustal carbonate rocks in the UFA. Pyrite exists in euhedral, massive and framboidal forms as a minor mineral the IAS and UFA. Hydrous ferric oxide (HFO) occurs mainly in the SAS, but also at a depth of more than 45 m where it is found together with pyrite. In the shallow subsurface SAS where the conditions are more oxygenated, As is likely bound to HFO, while in the deeper In the UFA where Fe and S are elevated As is likely predominantly in As-rich pyrite (Pichler and Mozaffari, 2015).

The exact mineralogical association of Mo in the sediments remains unclear. Although the mineral powellite ($CaMoO_4$) was observed in the aquifer matrix, it is unlikely that powellite is a primary mineral that precipitated during sediment deposition or early diagenesis. Instead the likely primary source for Mo is organic matter, which known to incorporate and concentrate Mo (e.g, Tribovillard et al., 2004). Organic carbon is present throughout all three hydro stratigraphic units, ranging from 0.1 to 3.3%.

Average annual rainfall in the study area is about 1.4 m/yr, with about 60% falling from June through September and estimates of groundwater recharge to the UFA ranged from 0.008 to 0.43 m/yr (Katz et al., 2009). Assuming most of the annual discharge in the Alafia River represents base flow groundwater discharge, mean daily recharge to the SAS (0.34 m/yr) can be estimated as equal to the mean daily flow of the Alafia River (9.41 m^3/s at the USGS #02301500 at Lithia, FL) divided by that drainage area at the gauge (868 km^2). This estimated recharge is similar to that obtained using the Thornthwaite method (0.24 m/yr) (Thornthwaite, 1948) and to the estimate of >0.25 m/yr which was used by Hughes et al. (2009) in their regional groundwater flow model.

The domestic supply wells with high As concentrations, were located up gradient from a series of 17 municipal supply wells (Fig. 1(a)). Average pumping rates at these wells were generally 10^{-2} m^3/s. But rates at individual wells varied widely, both at a single well on different days and between wells on a given day, as pumping is redistributed across the well field on a daily basis; over a 1–2 week period the daily pumping rate at any given well typically varies from zero to about twice it's average value. Among the wells nearest to the highest As concentrations, net pumping similarly varied over time which, in conjunction with seasonal fluctuations in precipitation (e.g., average summer monthly precipitation of about 20 cm is about twice that during the winter months), resulted in temporal variations in hydraulic heads of 5 m or more.

3. Methods

From the original Florida Department of Environmental Protection (FDEP) survey of 100 domestic wells in Lithia, approximately 40 were selected for further study. Those wells covered that same geographic region and range of As and Mo concentrations. Only limited well logs were available for the domestic supply wells and hence in most cases well depth and screened intervals are poorly constrained. To supplement the domestic supply well samples, the DEP installed five monitoring well clusters (DEP-1, DEP-2, DEP-3, DEP-4 and DEP-5), each cluster consisting of four wells, each with a screened interval of 6 m length at a different depth. Screened intervals were completed at depths of approximately 44 m in the IAS, near the IAS/UFA boundary at 62 m, and two intervals in the UFA at depths of 77 m and 90 m below surface (Fig. 1(b)). In each well the shallowest monitoring well was in the IAS and the lower three were in the UFA. The cluster locations were chosen to reflect the geographical coverage of the domestic wells. The cluster DEP-5 was installed away from the area of high As to serve as a control site. In order to test (1) if infiltration of water from a phosphate mine located about 3 km to the east of the domestic supply wells or (2) if infiltration of shallow groundwater (<10 m) could be the source of As to the domestic wells, eight shallow groundwater samples were collected by push core using a Geoprobe system (Fig. 1(b)).

3.1. Well sampling and chemical and stable isotope analyses

Water samples were collected from the domestic supply wells (DSW), the five DEP well clusters and the push core wells (PCW) following NAWQA and FDEP protocols (Koterba et al., 1995). Each well was purged a minimum of three casing volumes and water samples were collected after field properties (temperature, pH, specific conductance, turbidity, and dissolved oxygen) had stabilized. Water levels were taken prior to sampling.

Sulfide was determined in the field on a Hach DR 2800 VIS Spectrophotometer. Total As was analyzed by hydride generation-atomic fluorescence spectrometry (HG-AFS) on a PSA Millennium instrument following established procedures (Price and Pichler, 2006). A 2% solution of potassium iodide was used to reduce As(V) to As(III) prior to hydride generation. Molybdenum (Mo) was determined on a Perkin Elmer Optima 2000 DV inductively coupled plasma − optical emission spectrometer (ICP-OES). Accuracy and precision were verified through the use of internal and external standards (NIST Trace Elements 1643e) and 10% duplicate measurements. All other chemical parameters were analyzed in the certified laboratory of the DEP by a combination of ion chromatography, ICP-OES and ICP-MS.

The stable oxygen and hydrogen isotopes were determined by simultaneous analysis of $^{18}O/^{16}O$ and D/H isotope ratios using an LGR DLT-100 instrument (Los Gatos Research, Inc., Mountain View, CA, USA). Each sample was injected 6 times, with the first 3 injections discarded to eliminate memory effects, and the average of injections 4, 5 and 6 used for isotope ratio calculations. Working standard waters calibrated against NIST standard reference materials (VSMOW, GISP, SLAP) were inserted in the sample sequence (usually before and after each group of six unknowns). Results are given in delta notation ($\delta^{18}O$ and δD) relative to Vienna Standard Mean Ocean Water (VSMOW). Precision was better than 0.3‰ and

0.8‰ for $\delta^{18}O$ and δD, respectively.

3.2. Tritium–Helium dating

The ^3H–^3He dating method has been used in many groundwater studies (e.g., Solomon and Cook, 2000). All DEP monitoring wells, all Geoprobe samples (PCW) and 20 DSW were sampled for groundwater dating. The samples were collected (in duplicate) in pinched-off copper tubes. The sample fraction to be used for tritium determination by helium ingrowth was collected in duplicate into 500 mL glass bottles with polycone seals.

Analysis of ^3H, He isotopes for ^3H–^3He dating was conducted at the noble gas laboratory of the Institute of Environmental Physics, University of Bremen following the method detailed in Sültenfuß et al. (2009). For groundwater samples, the precision of the He concentrations was better than 1%. The detection limit for ^3H was 0.01 TU (tritium units, 1 TU = 10^{-18} $^3H/^1H$), which allowed the detection of the residue of pre-bomb ^3H. The uncertainty was typically less than 3% for samples of >1 TU and 0.01 TU for very low concentrations. For ideal samples, analytical conditions allow a time resolution of about 3 months for apparent ages of less than 10 years. Unknown hydrogeological conditions affecting gas exchange, such as inaccurate temperatures assumed for gas exchange with the atmosphere (Solomon et al., 1992), lead to an effective time resolution of about 0.5–1.0 year. More details of the sampling, analysis and data evaluation of the method are given elsewhere (Sültenfuß et al., 2009).

3.3. Hydrogeological modeling

To determine if the variations in pumping and recharge could account for the mixing of shallow and deep groundwater, regional groundwater flow was simulated using the United States Geological Survey's three-dimensional groundwater flow model MODFLOW (Harbaugh, 2005). The modeled region encompassed a 20 km wide swath centered about the east-to-west flowing Alafia River and extending 43.5 km from the Alafia River drainage divide in the east to the shores of Tampa Bay in the west (Fig. 1(a)). Groundwater flow in the region generally follows the regional westward dipping topographic gradient, but is locally diverted toward the dominant topographic feature of the region, the Alafia river valley. The highest As concentrations were located on the southern rim of the valley, about 10 m above the valley floor and about 30 km upstream from the river outlet at Tampa Bay.

Our hydrogeological model was adapted from the regional flow model presented by Hughes et al. (2009) and consists of three hydro stratigraphic units: i) the Surficial Aquifer System (SAS); ii) the Intermediate Aquifer System (IAS); and iii) the Upper Floridan Aquifer system (UFA). The hydraulic conductivity of each layer is similar to that used by Hughes et al. (2009), although for simplicity, and in contrast, we assume the hydraulic conductivity is isotropic (Table 1). Model hydraulic conductivities are consistent with direct measurements of hydraulic conductivities in these units as summarized by the Southwest Florida Water Management District (Arthur et al., 2008) and well tests of from a public water supply well located about 35 km northwest of the domestic supply wells (Stewart et al., 1978).

In the model the SAS was discretized into two layers, the IAS into five equally thick layers, and the UFA into seven equally thick layers. Horizontally, within the zone of highest As concentrations all layers were discretized into square elements 100 m on a side, with the element dimensions slowly increasing to no more than 1 km with increasing distance from the high As concentrations. For each layer there were a total of 3465 elements, and a total of 45,045 elements overall. All model edges are no flow boundaries except along Tampa Bay, where the head was set to mean sea level. Rivers were modeled as drains and steady-state heads were solved using MODFLOW's pre-conditioned conjugate gradient solver.

Table 1
Hydrogeologic model parameters.

Hydraulic Conductivity	**K** (m/day)
Surficial Aquifer System (SAS)	4
Intermediate Aquifer System (IAS)	
Outside Private Well Area	0.36
Within Private Well Area	36
Upper Floridan Aquifer (UFA)	36
Alafia River bottom conductance	103
Recharge	**R** (m/yr)
	0.34
Well Pumping Rates	**Q** (m^3/day)
SC1-3	8242
SC4-6	15,367
SC7-10	19,228
SC11-12	10,596
SC13	6848
SC14	6571
SC15	6462
SC16	5543
SC17	6315

Well construction notes indicated that most of the private wells were either unlined or screened at multiple levels. Thus each open borehole creates a pathway for vertical flow that significantly enhances the effective vertical permeability of the aquifer, particularly across the IAS. Further, because the IAS is composed of alternating layers of more and less permeable rocks and sediments (Arthur et al., 2008), the enhanced vertical permeability makes it easier for flow to access the high permeability layers within the IAS, increasing the bulk effective horizontal permeability of the IAS. Although the actual increase in permeability due to the high density of private wells depends on the details of the hydro stratigraphy and well construction, the increase can be estimated by modeling flow within the domestic supply wells as a series of parallel pipes. For n wells of radius r uniformly distributed over an area A, the net hydraulic conductivity is

$$K = K_{matrix} + \frac{n\rho g \pi r^2}{2\mu A} \quad (1)$$

where ρ and μ are the density and dynamic viscosity of water, g the gravitational acceleration and K_{matrix} the hydraulic conductivity of the formation without any wells. Within the zone of highest As concentrations, there are ~100 wells in a 2.5 km × 1.5 km region. Assuming a typical domestic well diameter of 10 cm, the net effective vertical hydraulic conductivity of the well network (~55 m/day) is about two orders of magnitude greater than the permeability of the intact IAS (0.36 m/day).

To investigate the possible impact of the high density of wells on groundwater flow paths, in some model simulations we increased the hydraulic conductivity by two orders of magnitude within a 2.5 km × 1.5 km region centered over the region of highest private well density. As noted above, because increasing the vertical permeability in the IAS also increases the effective horizontal permeability, the zone of increased hydraulic conductivity was assumed isotropic. Although not fully explored here, in general greater anisotropy in the increase in hydraulic conductivity should result in less mixing between the IAS and UFA waters.

4. Results

4.1. Well-water

The major anion and cation composition of water samples from the DEP and monitoring wells are summarized in Table 1S (Supporting Material). The elevated pH of 9.4 in sample DEP-1-165 indicates a minor grout problem (Barcelona and Helfrich, 1986), but should have only little influence on the measured parameters, other than HCO_3, Ca, and Mg. In the DEP samples, phosphate, total Kjeldahl and inorganic nitrogen were low, indicating little to no agricultural influence in the deeper well samples. In general, except for two samples, the major ion composition of the well water samples were as expected for Floridan groundwater (compare to Jones and Pichler, 2007; Pichler, 2005; Sacks and Tihansky, 1996). The exceptions were samples PCW-2 and PCW-3, which were collected from the SAS next to the settling pond of the phosphate mine located about 3 km to the east of the study area and which showed a strong evaporative enrichment as evidenced by their $\delta^{18}O$ and δD values and elevated concentration of dissolved solids (Table 1S (Supporting Material)). Nevertheless, they had less than 3 μg/L Mo and 2 μg/L As (Table 1S (Supporting Material)). Since they were not enriched in As and Mo and were collected to the east of Thirty Mile Creek (Fig. 1), a likely hydrogeological barrier in the SAS, they were excluded from further discussion.

In the remaining samples only those elements sensitive to changes in redox conditions, including sulfide, oxygen, iron and arsenic, showed significant variations, particularly with depth. Dissolved oxygen levels (DO) in the shallow wells (PCW) tapping the SAS (2.88 ± 2.65 mg/L; mean ± standard deviation) were higher than in the DEP monitoring wells which are screened in the deeper IAS and UFA (0.22 ± 0.21 mg/L). Dissolved oxygen levels in the PCW were also higher than in the DSW (0.69 ± 1.10 mg/L). Using a two-sample t-test assuming unequal variances, the difference in dissolved oxygen levels between the shallow groundwater samples and the domestic supply well samples was statistically significant ($p = 0.05$) as is the difference between the shallow groundwater samples and the DEP well samples ($p = 0.002$).

With a few exceptions oxygen reduction potential (ORP) values were higher in samples from the SAS and lower in the IAS and UFA samples. If the single anomalously reduced sample from the IAS from DEP-5 is excluded, ORP values were significantly lower (two-tailed unequal variance t-test $p = 0.3$) in the UFA compared to those in the IAS. Consistent with the general decrease in ORP with depth, sulfide concentrations consistently increased with sample depth (Table 1S (Supporting Material)).

Arsenic and Mo were well above the US EPA recommended values in samples from the screened interval in the IAS in wells DEP-1, DEP-2 and DEP-3 (Fig. 2, Table 1S (Supporting Material)). These wells are located in the center of the study area, which also showed the highest As and Mo concentrations in the domestic supply wells (DSW) (Fig. 1). Among samples from the DEP wells, a statistically significant ($p > 0.004$) negative log-linear correlation exists between sulfide and As ($p < 0.004$) and between sulfide and Mo ($p < 0.001$). Among the monitoring well samples, a statistically significant negative log-linear correlation also exists between sulfide and As ($p = 0.02$), but not between sulfide and Mo ($p = 0.62$).

The DSW were sampled in May 2008 and resampled in April 2009. Most chemical and physical parameters remained stable for that period of time, although there seems to be a systematic error in Na concentrations, because all samples collected in May 2008 had a substantially lower concentration, while other major cations and anions did not change (Table 2S (Supporting Material)). Aside from Na, the only chemical parameters with significant variation between the two sampling periods are the redox dependent parameters As, S, ORP, and, to a lesser extent Mo, which is less sensitive to redox conditions than As, S, or ORP. Arsenic concentrations in the domestic supply wells range from 0.1 to 370 μg/L and Mo concentrations from 0.3 to 4740 μg/L (Table 2S (Supporting Material)). There is no statistically significant linear correlation between sulfide and As. Some of the sulfide values in the domestic supply wells are as low as those measured in the monitoring wells.

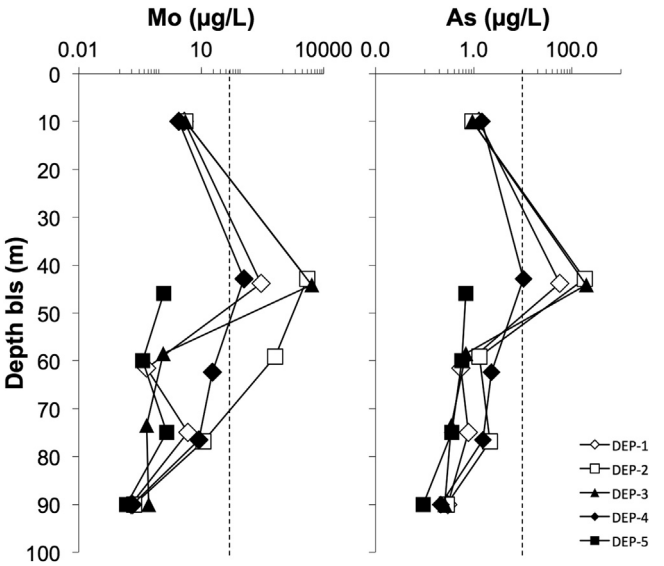

Fig. 2. Depth profiles for the concentration of arsenic (As) and molybdenum (Mo) in groundwater collected at the 4 monitoring levels of the multi-level monitoring wells DEP-1 to DEP-5 and at the shallow push core wells next to the DEP clusters. The dashed line indicates the US EPA MCL for As of 10 μg/L and the recommended (but not enforced) MCL for Mo of 40 μg/L.

The values for oxygen and hydrogen isotopes fall on the local meteoric water line (LMWL) for central Florida (Fig. 3) (Kendall and Coplen, 2001). Along the LMWL the DEP samples are distributed between two apparent end members; shallow groundwater, which has an isotopic composition similar to the mean composition of precipitation, and deep groundwater. There is no significant correlation between $\delta^{18}O$ and As or Mo, although those samples with high As and Mo concentrations generally have an isotopic

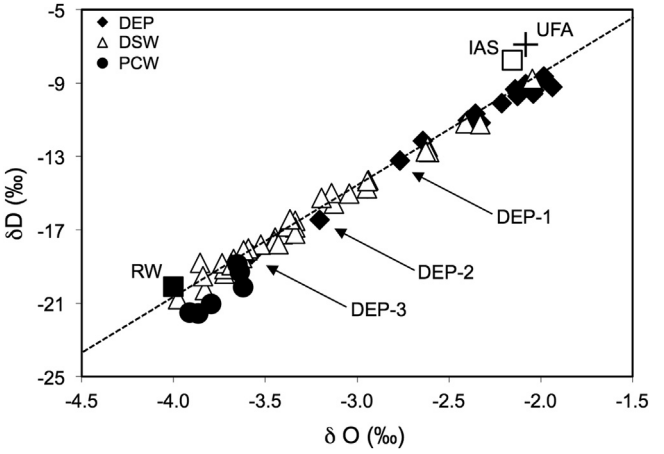

Fig. 3. Isotopic composition of Lithia area groundwater samples collected at the domestic wells, DEP monitoring wells and PCW wells. The dashed line indicates the local meteoric water line (LMWL) from Kendall and Coplen (2001). RW is the isotope value for the mean annual weighted rainfall in central Florida and IAS and UFA are values reported for the intermediate und upper Floridan aquifer (Sacks and Tihansky, 1996).

composition that are a mixture of shallow and deep groundwater, with the highest As and Mo concentrations being more similar to deep rather than shallow groundwater.

4.2. ^{3}H–^{3}He age dating

The distribution of ^{3}H–^{3}He groundwater ages for 20 DEP samples, 13 DSW samples, and 6 PCW samples are listed in Table 2 and displayed in Fig. 4. In general the calculated ages correlate with depth. All shallow groundwater samples have ages less than 40 years, with most between 20 and 30 years. The average age of the shallow groundwater samples is 28 ± 2 years (mean ± standard error). All the shallow groundwater samples had ^{3}H concentrations >1.8 TU and were free of radiogenic ^{4}He. The high ^{3}H concentrations were consistent with ^{3}H concentrations in precipitation since 1955, which have been >1 TU. In contrast, all DEP samples from the screened intervals in the UFA (depths >70 m) had ages >50 years. The ^{3}H concentrations in those samples were all less than 0.03 TU, or less than 1% of the concentration of ^{3}H in precipitation since 1955, thus excluding the addition of younger water to those depths.

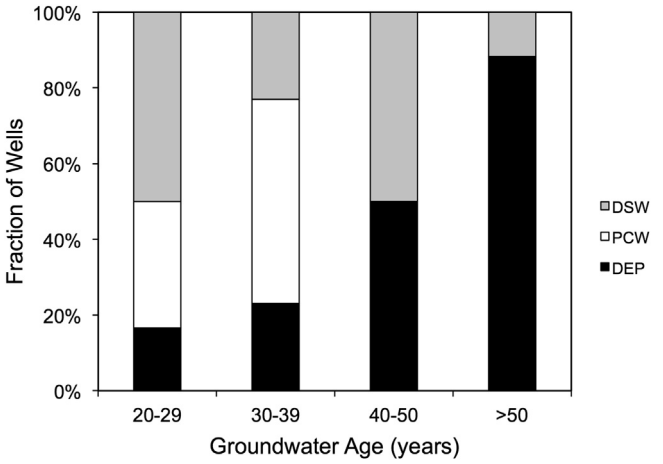

Fig. 4. Distribution of groundwater ages for the three types of wells sampled.

Table 2
Tritium (^{3}H) and helium (^{3}He) ages.

Sample ID	Aquifer System	Depth m	^{3}H TU	^{3}H–^{3}He TU	Age Years
1-165	IAS	44	0.56	5	40
1-225	UFA	62	0	0.5	>50
1-270	UFA	75	0	0	>50
1-320	UFA	90	0	0.5	>50
2-163	IAS	43	1.25	3.7	30
2-217	UFA	59	0.18	0.5	20
2-276	UFA	77	0	0	>50
2-320	UFA	90	0	0	>50
3-167	IAS	44	0.78	3.7	30
3-215	UFA	59	0	0	>50
3-265	UFA	74	0	0	>50
3-320	UFA	90	0	0	>50
4-163	IAS	43	0.03	0	>50
4-228	UFA	62	0	0	>50
4-275	UFA	77	0.03	0	>50
4-320	UFA	90	0.02	0	>50
5-173	IAS	46	0.11	0.6	32
5-220	UFA	60	0.02	0	>50
5-270	UFA	75	0	0	>50
5-320	UFA	90	0	0	>50
PCW-1	SAS	9	2.1	9.2	30
PCW-2	SAS	9	2.22	7.4	26
PCW-3	SAS	9	1.85	n.d.	n.d.
PCW-4	SAS	9	3.6	23.3	38
PCW-5	SAS	9	1.9	4.2	21
PCW-6	SAS	9	2.5	10.4	30
PCW-7	SAS	9	2	n.d.	n.d.
PCW-8	SAS	9	2.1	6.4	25
01-09	n.k.	n.k.	1.25	16.5	46
03-09	n.k.	n.k.	1.55	n.d.	n.d.
09-09	n.k.	n.k.	1	5.6	33
11-09	n.k.	n.k.	1.63	9	33
12-09	n.k.	n.k.	0.17	1	32
13-09	n.k.	n.k.	1.4	10.5	38
15-09	n.k.	n.k.	0.65	13	54
16-09	n.k.	n.k.	0.5	n.d.	n.d.
18-09	n.k.	n.k.	2.2	n.d.	n.d.
19-09	n.k.	n.k.	2.55	n.d.	n.d.
39-09	n.k.	n.k.	0.13	n.d.	n.d.
20-09	n.k.	n.k.	0.65	n.d.	n.d.
21-09	n.k.	n.k.	0.5	2.6	30
22-09	n.k.	n.k.	1.25	2.7	20
23-09	n.k.	n.k.	0.86	n.d.	n.d.
26-09	n.k.	n.k.	0.04	n.d.	n.d.
27-09	n.k.	n.k.	0.85	5	35
30-09	n.k.	n.k.	1.5	11.5	38
36-09	n.k.	n.k.	0	0	>50
38-09	n.k.	n.k.	0.65	2.25	27

Note: The Sample ID is consistent with those in Tables 1S and 2S and n.d. indicates that measurements could not be performed and n.k. indicates not known. For the abbreviations IAS, UFA and SAS please see text.

The ^{3}H–^{3}He groundwater ages for the domestic supply wells (DSW) were generally intermediate between the shallow groundwater ages and those of the DEP samples from the screened intervals in the UFA. The average age of the DSW samples was 35 ± 3 years. ^{3}H concentrations are variable, ranging from 0 to 2.6 TU, with a mean of 1 TU and a coefficient of variation of 0.7. Four of the 13 DSW samples contained significant radiogenic ^{4}He. Values of radiogenic ^{4}He are an indicator for old water and typical ages derived from such ^{4}He values are some hundreds to some thousands years in age. But the DSW samples also contained significant concentrations of ^{3}H (0.65–1.63 TU), indicative of water ages of a few decades or less. The presence of both significant ^{3}H and ^{4}He in these wells can only be explained by mixing between very old and younger waters.

4.3. Water levels

The water levels in the DEP wells were measured five times from April 2008 to April 2009 and water levels varied by about 4.5 m. This variation was largely seasonally driven, because water levels were highest at the end of the rainy season in October and lowest at the end of the dry season in June. If the surficial wells undergo the same water level fluctuations remains unknown, because they were measured only in April 2009. Within each of the well clusters DEP-1 to DEP-4, water levels in the shallow interval (IAS) were consistently 1–2 m higher than in the deeper intervals (UFA), indicating generally downward flow between two different aquifers (Fig. 5).

The water levels for all monitoring depths increased roughly from west to east, consistent with both the regional flow direction and increasing distance from the center of the municipal well field to the west of the study area (Fig. 1). In Fig. 5 the DEP monitoring well clusters are plotted with increasing distance from the municipal well SC-12 (Fig. 1(a)). The water levels across our study area in the IAS (topmost screened interval of the DEP wells) increased from west to east by almost 4 m in the IAS and by more than 2 m in the UFA. Well DEP-5, which was the As- and Mo-free control well, underwent exactly the same yearly changes as all other DEP wells (Fig. 5(a)) and had the lowest water levels in all of its monitoring intervals. It is noteworthy, however, that in this well, which is closest to the municipal well field, the difference in head

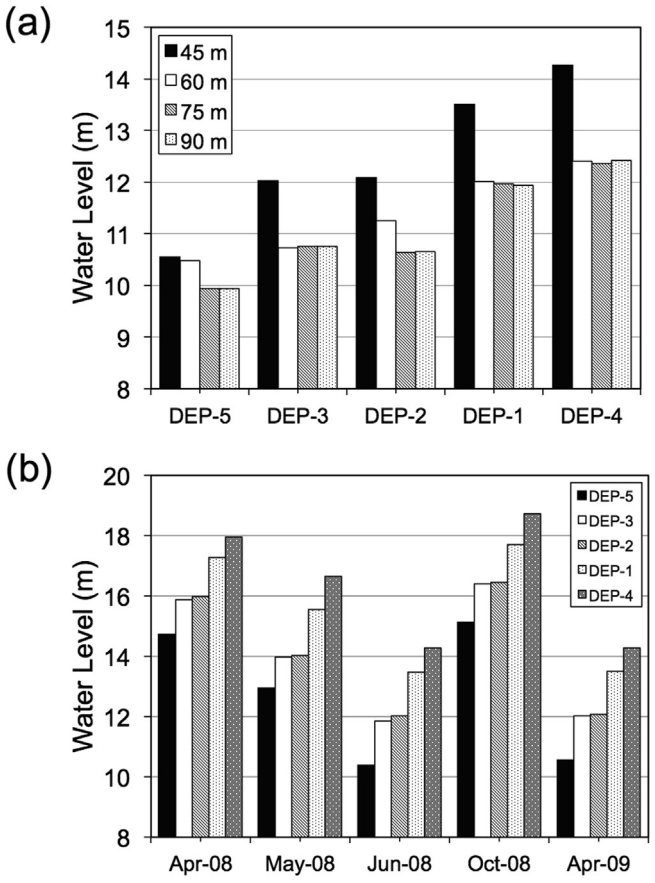

Fig. 5. (a) Water levels in April, 2009 for each monitoring depth relative to the National Geodetic Vertical Datum of 1929 (NGVD) for the DEP well clusters. (b) Water levels for the 45 m screen from April 2008 to April 2009. Note: The well clusters are ordered in progressive distance from municipal supply well SC-12 (Fig. 1a).

between the IAS and the UFA was much less than in the other DEP wells nearer the high As and Mo concentrations. In fact, the vertical hydraulic gradient, calculated from the difference head between the uppermost and lowermost screened intervals, consistently increases with increasing distance from the well field and is a factor of four larger in DEP-4 (the furthest well cluster) than in DEP-5 (the closest). This is counter to what we would expect if pumping from the municipal well field was the dominant control on the hydraulic gradients, because gradients, including vertical gradients, should increase closer to the pumping. Note also that among the wells in the high As region, in well DEP-2 only, which is located in the middle of the highest density of DSW (Fig. 1), the head at the IAS/UFA boundary (~60 m depth) was about three quarters of a meter higher than the heads in the UFA (deepest two screened intervals). Elsewhere in this region the head at the IAS/UFA boundary was similar to that in the deeper UFA. This indicates a reduced vertical hydraulic gradient across the IAS in the region of highest DSW density.

4.4. Hydrogeological modeling

Fig. 6 compares the modeled heads with all wells pumping at their average rate to head measured in October, 2008. The model fits the observed heads well (average RMSE = 0.5 m), particularly given that the permeabilities were set *a priori* and thus were not calibrated values.

Cross sections showing groundwater flow paths in the region of

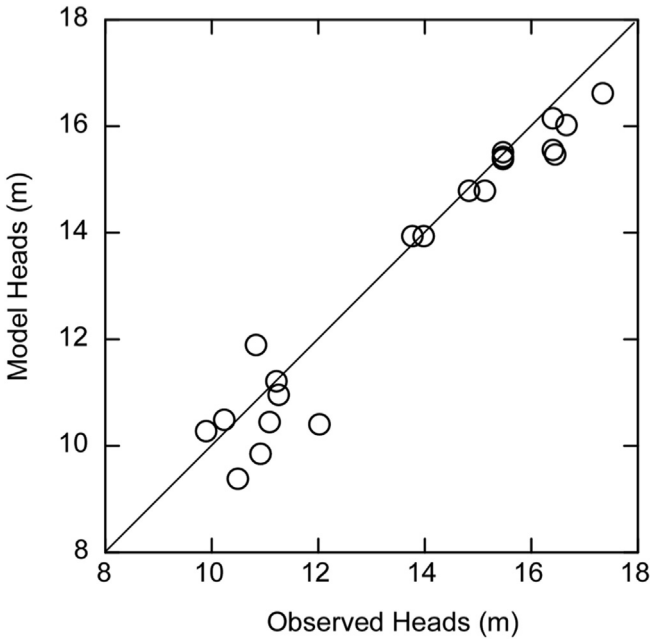

Fig. 6. Comparison of modeled hydraulic heads with all wells pumping at their average rate to hydraulic heads measured in October, 2008.

the highest As concentrations are shown in Fig. 7. Steady state groundwater flow paths with all municipal wells pumping at their average rate are shown in panel (a). Consistent with the general pattern of regional groundwater flow in horizontally layered aquifer systems (Freeze and Witherspoon, 1966), flow is downward and near vertical across the IAS confining unit, with little to no mixing of shallow and deeper waters within the IAS.

The steady state groundwater flow paths with the six municipal supply wells nearest the high As concentrations turned off (no pumping) are shown in panel (b) of Fig. 7 and are virtually identical to those conditions when all the wells are pumping (Fig. 7(a)). Thus while changes in pumping and recharge change the rate of groundwater flow, they do not significantly alter flow paths. This indicates that changes in the rates of pumping of the municipal supply wells are not a direct cause of long term mixing of shallow and deep waters. However, pumping does affect the vertical hydraulic gradients across the IAS; steeper gradients are required to supply more water to the wells during pumping. Along the flow paths shown in Fig. 7(a),(b), the increase in vertical hydraulic gradient due to the onset of pumping is a few percent or less. Closer to the municipal supply wells pumping increases the gradient in the region of highest As concentrations by up to about 30%. As groundwater velocity is linearly related to hydraulic gradient, a corresponding increase in flow rate occurs with the onset of pumping. We note that this prediction of increasing vertical hydraulic gradients across the IAS closer to the municipal wells is inconsistent with the observed gradients; among the DEP wells in the region of high As concentrations, the greatest vertical hydraulic gradient across the IAS occurs in DEP-4, the well located furthest from the municipal well field.

Fig. 7(c) shows the flow paths in the region of highest As concentrations when the permeability in this region is increased to account for leakage along the domestic well boreholes. Near the up gradient boundary of the zone of increased permeability, groundwater is drawn up from the deeper UFA into the IAS, where it then flows near groundwater percolating directly down from the upper SAS. Within the complicated hydro stratigraphy of the IAS and with

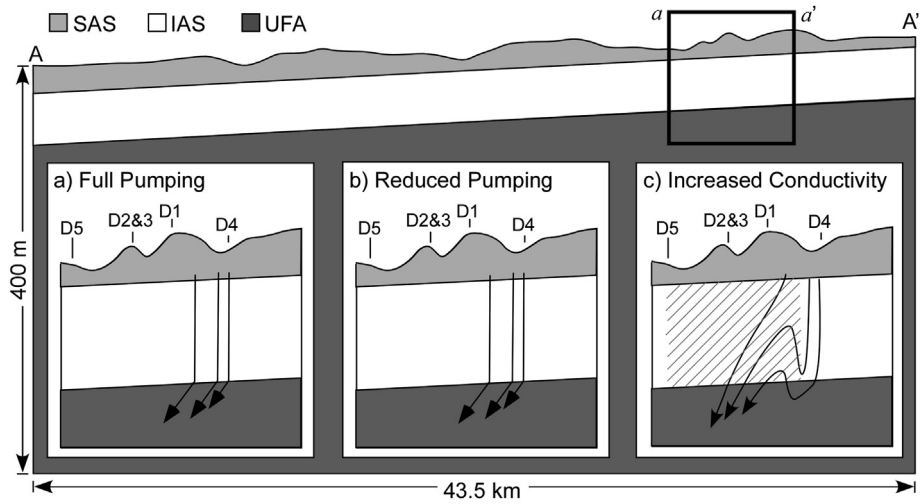

Fig. 7. Cross-section of the modeled region with inset showing groundwater flow paths along the section a–a′ for: a) all municipal wells pumping at their average rate, b) the pumping set to zero for the six wells nearest the region of high As concentrations, and c) with the permeability increased by two orders of magnitude within the hatched region of the IAS due to the high density of open wells. Steady state low paths are largely insensitive to changes in pumping, but are consistent with the mixing of deep and shallow groundwater when the permeability locally increases. The location of the cross section is also indicated by the dashed line (a–a′) in Fig. 1(c). The labels D1-D5 indicate the locations of the five DEP monitoring wells.

interlayer flow facilitated by the open wells, it is likely that this convergence of flows from the shallow and deep aquifers results in the mixing of upwelling waters from the UFA with downward percolating water from the SAS. The upwelling of waters from the UFA to the IAS is facilitated by a reduced, and in some places even reversed, vertical hydraulic gradient across the IAS in the high density well zone, consistent with the reduced vertical hydraulic gradient observed in well DEP-2.

These results indicate that the increased permeability created by the high density of open domestic well boreholes results in changes in flow paths that permit the mixing of shallow and deep groundwater. The complicated flow paths shown in Fig. 7(c) reflect an intricate suite of changes to hydraulic head gradients, including local reversals of the vertical gradient. In general, however, the magnitudes of the greatest downward vertical hydraulic gradients are much lower than for the case of a homogeneous IAS and no pumping. However, with respect to flow velocities, the impact of the lower head gradients is offset by the increased hydraulic conductivity, which is two orders of magnitude larger than in the homogeneous case. Thus the fastest downward flow velocities in the high well density region are an order of magnitude or more faster than in the homogeneous IAS condition. That is, locally increasing the permeability of the IAS not only alters the flow paths and enhances mixing of shallow and deep waters in the IAS, but also dramatically increases the fastest flow rates through the IAS by an order of magnitude or more.

Interestingly, flow paths consistent with significant mixing of shallow and deep groundwater were not observed when the permeability within the zone of highest As concentrations was only increased an order of magnitude (as opposed to the two order of magnitude increase between the simulations shown in Fig. 7(a) and (c)). Nor was mixing apparent when only the vertical permeability within the high well density zone was increased. Thus mixing may require both a critical density of wells and also that the wells provide access to more permeable horizontal layers that thereby increase both the effective vertical and horizontal permeability.

5. Discussion

Despite the relatively small area, the geochemical and hydrogeological setting in Lithia is complex, consisting of: i) extensive cyclical pumping in the well field to the west, ii) large seasonal changes in hydraulic head, ii) multiple aquifers with different hydraulic heads, and iv) a large density of domestic supply wells (DSW). Despite this complexity, the observed As mineralogy followed the expected redox gradient for downward groundwater flow from the oxygenated near surface to more and more reducing conditions at depth. HFO, which is generally stable under oxygen-rich conditions (Jambor and Dutrizac, 1998), was found mainly in the SAS, while pyrite, which is stable under the reduced conditions (e.g., Jones and Pichler, 2007), was found mainly in the UFA (Pichler and Mozaffari, 2015). In such a poised system, any perturbation to groundwater flow pathways that results in a change in redox state will mobilize As. Thus as at other sites with high groundwater As concentrations (e.g., Amini et al., 2008; Ferguson and Gavis, 1972; Korte and Fernando, 1991; McNeill et al., 2002; Peters and Blum, 2003), at Lithia it is likely that the high dissolved As and Mo concentrations in the DSW were the result of hydrogeological conditions, particularly the mixing of shallow and deep groundwater, which caused the mobilization of those metals, but have not yet flushed them from the aquifer. Below we first summarize the hydrogeological conditions driving the mixing of shallow and deep groundwater and then summarize the isotopic evidence consistent with the mixing of shallow and deep groundwater. Finally we explore how groundwater mixing might cause the release of both As and Mo.

5.1. Shallow and deep groundwater mixing

The enhanced permeability created by the high density of open-hole domestic supply wells (DSW) creates two distinct types of shallow and deep groundwater mixing (Fig. 7(c)). Near the up gradient boundary of the region of high well density, deeper, more reduced waters from the UFA are drawn upwards into the IAS. Further down gradient the flow of this upwelling water reverses and it returns to the UFA. Since this return flow is in addition to recharge from the overlying SAS, and since recharge from the SAS to the UFA is reduced over the zone of upwelling, mass balance requires that the downward vertical flow of oxygen-rich shallow groundwater from the SAS to the IAS and UFA be enhanced near the

center of the zone of high-density DSW. Down welling flow velocities will by further increased by pumping, both locally from the DSW and regionally from the municipal supply wells. In both cases (upwelling at the up gradient boundary and down welling in the central part of the zone of high density domestic supply wells), the local scale mixing of shallow and deep groundwater would be facilitated by the highly heterogeneous and anisotropic permeability created by the intersection of the DSW boreholes and the naturally fracture network in the aquifer matrix.

The modeled mixing between SAS and UFA derived groundwater in the DSW was corroborated by the stable isotopic composition of the DSW. The $\delta^{18}O$ and δD isotopic composition of the DSW generally fell on a mixing line between shallow and deep groundwater (Fig. 3). High As and Mo concentrations were exclusively found in those DSW, which plot between the shallow and deep end-members, indicating that the high As and Mo values are associated with the mixing of shallow and deep groundwater. Mixing between shallow and deep groundwater, which generally have a high and low oxygen reduction potential (ORP), respectively, should produce a groundwater with an intermediate ORP (e.g., Carucci et al., 2012) and beneath Lithia, particularly those samples with an intermediate ORP showed elevated As and Mo concentrations (Fig. 8). The mixing of groundwater was also indicated by the radiogenic isotopic composition of the DSW. As noted above, 4 of the 13 DSW samples had significant radiogenic ^{4}He, indicative of water ages of hundreds of year or more, and significant concentrations of ^{3}H (0.65–1.63 TU), indicative of water ages of a few decades or less (e.g., Plummer et al., 2000). The presence of both significant ^{3}H and ^{4}He in these wells can only be explained by mixing between very old and younger waters. Mixing between deep (old) and shallow (young) groundwater was also implied by comparing their ^{3}H composition to $\delta^{18}O$. In central Florida as well as most other groundwater systems shallow groundwater generally has lighter $\delta^{18}O$ values and higher TU (e.g., Katz et al., 2007). In the study area water samples from the deepest three screened intervals of the DEP well clusters had low TU values, but heavier $\delta^{18}O$ values (Fig. 9(a)), while the shallow monitoring wells (PCW) generally had high TU values, but low $\delta^{18}O$ values (Fig. 9(b)). The DSW occupied more or less the space between the PCW and deep DEP samples (Fig. 9(c) and (d)).

The results from the hydrogeological modeling and isotopic analyses can be summarized as follows. The enhanced permeability provided by the high density of DSW is sufficient to alter the groundwater flow paths beneath Lithia in such that in some locations deeper, anoxic UFA groundwater can flow up into the shallower IAS while at other locations oxygen-rich shallow groundwater from the SAS can flow directly into the deeper, nominally anoxic IAS and UFA aquifers. Within the complicated hydro stratigraphy of the IAS and with interlayer flow facilitated by the open wells, it is likely that shallow and deep groundwater mix where upwelling water from the UFA meets down welling water from the SAS – in the IAS. Depending on water use from the DSW, seasonal changes and potentially varying pumping rates in the well field to the west, flow directions likely oscillate and thus cause successions of oxic and anoxic conditions in the IAS.

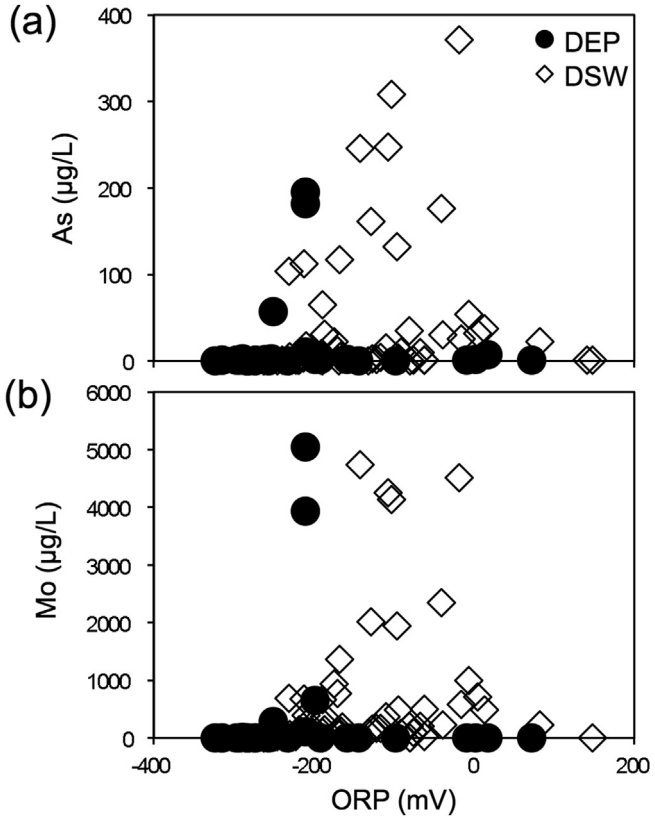

Fig. 8. (a) Relationship between oxygen reduction potential (ORP) and As in the monitoring well clusters 1 to 5 (DEP) and the domestic supply wells (DSW). (b) Relationship between ORP and Mo in the monitoring well clusters 1 to 5 (DEP) and the domestic supply wells (DSW).

5.2. *Mobilization of As and Mo*

The isotopic compositions of the groundwater samples clearly demonstrated mixing of shallow and deep water and the hydrogeological modeling indicated that this mixing is associated with the enhanced permeability of the IAS created by the high density of DSW and that the redox conditions change back and forth between oxic and anoxic.

In central Florida and in the study area As has been found as impurities in three different minerals; pyrite, hydrous ferric oxide (HFO) and powellite (Lazareva and Pichler, 2007; Pichler and Mozaffari, 2015; Pichler et al., 2011; Price and Pichler, 2006), while Mo was found in the form of powellite ($CaMoO_4$) or was loosely adsorbed onto sediment grains, mineral surfaces or organic matter within the aquifer matrix (Pichler and Mozaffari, 2015). Powellite, however, is not considered primary source of Mo, because based on observations by transmitted light and scanning electron microscopy it was identified as the last mineral phase to precipitate in the aquifer matrix (Pichler and Mozaffari, 2015). Thermodynamic modeling with the computer code GWB, using recent thermodynamic data for aqueous Mo species and powellite (Essington, 1992; Felmy et al., 1992) showed that powellite was super-saturated in all groundwater samples in the study area that had Mo concentrations above 2000 µg/L. The most likely primary source for Mo is thus organic matter, which is abundant in the aquifer matrix beneath Lithia (Pichler and Mozaffari, 2015) and known to incorporate and concentrate Mo (e.g, Tribovillard et al., 2004). The mobilization and fate of As and Mo however seem to be more difficult than simple oxidation of organic matter or pyrite, because of the apparent redox disequilibrium in the IAS in the study area, i.e., co-occurrence of pyrite and HFO and pyrite and powellite in the aquifer matrix (Pichler and Mozaffari, 2015). Thus, following an initial release from the aquifer matrix, As and Mo could be adsorbed or co-precipitated by either powellite, pyrite or HFO under uncertain redox conditions and later released from either (e.g., Alberic and Lepiller, 1998; Amirbahman et al., 1997; Bostick and Fendorf, 2003; Bostick et al., 2003; Pichler et al., 1999; Welch and Lico, 1998), The stability of powellite is mainly

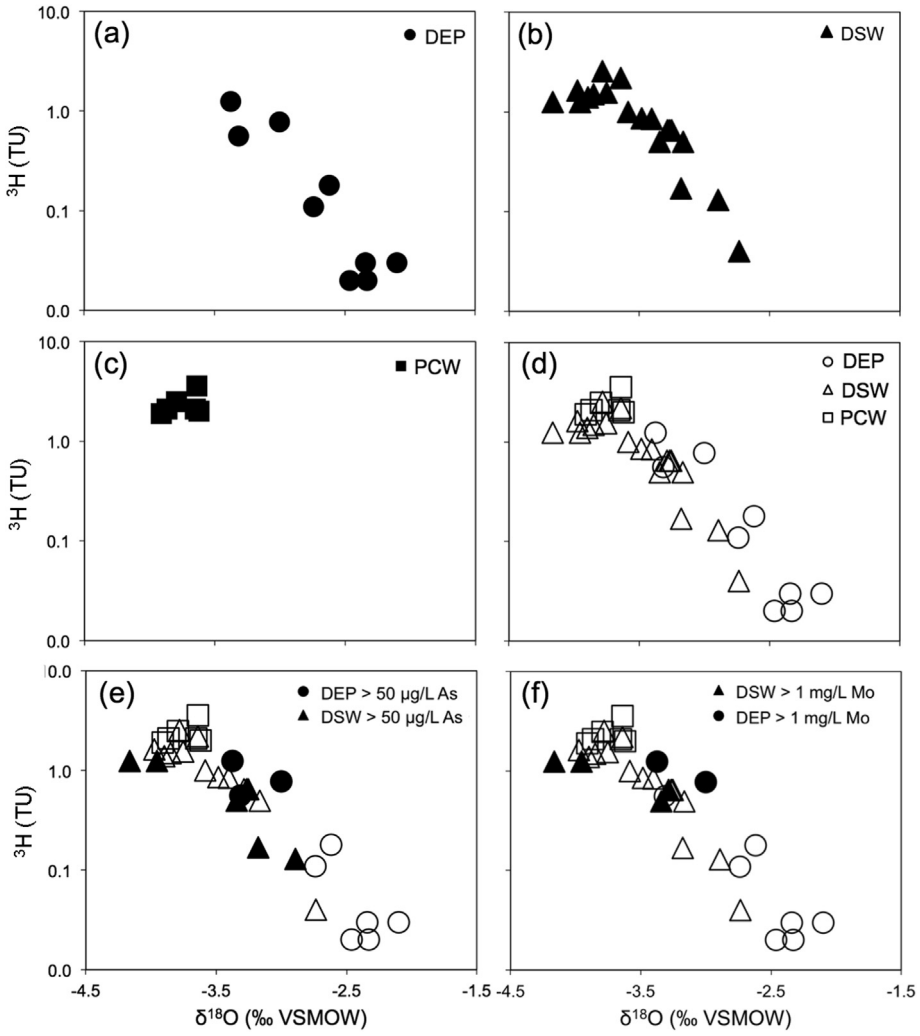

Fig. 9. Plots of 3H (TU) vs. $\delta^{18}O$ for the DEP wells (a), the shallow monitoring wells (b), the DSW (c), a combination of all sampled wells (d), a combination of all sampled wells where elevated Mo values are marked (e) and a combination of all sampled wells where elevated As values are marked (f). Those DEP wells, which have low 3H show relatively higher $\delta^{18}O$ values, while the shallow PCW samples have high ^{3}H, but show low $\delta^{18}O$ values. Those DEP and DSW samples high in As and Mo plot intermediate between position in the $^{3}H - \delta^{18}O$ diagram, a position, which can only be explained by mixing between the two endmembers, shallow groundwater (PCW) and deep groundwater (UFA).

controlled by the ion activity product (IAP) of Ca^{2+} and MoO_4^{2-} and thus, dissolution of secondary powellite is possible once its IAP would be less than its solubility product (K_{sp}) (e.g., Conlan et al., 2012). The importance of mixing for the release of As and Mo was also suggested by sulfide and ORP values, which are indicators of redox conditions. Only those wells, where sulfide and ORP values were intermediate between the two end-members had high As and Mo concentrations (Fig. 8). Thus we propose that the release of Mo to groundwater in the IAS intervals could be a combination of changing redox conditions and changing IAP due to mixing between shallow and deep groundwater, as well as the reversal from oxygenated to reducing conditions. The importance for mixing for the release of As and Mo is further indicated by the $\delta^{18}O$ and ^{3}H values of those samples high in As and Mo. High As and Mo concentrations were only found in those DSW and DEP samples, which intermediate $\delta^{18}O$ and ^{3}H values between those of the shallow and deep groundwater end-members (Fig. 9(e) and (f)).

The hydrogeological modeling suggests that in these regions the vertical downward flux of recharge is enhanced relative to that in the peripheral regions of high domestic well density. Enhanced downward flux would bring oxygen-rich shallow groundwater to the deeper IAS and UFA aquifers. Since shallow groundwater is more oxygenated (Table 1S (Supporting Material)) and thus has the potential to oxidize pyrite and organic matter, its introduction into the deeper aquifers should trigger the release of As and Mo from the aquifer matrix. Price and Pichler (Price and Pichler, 2006) found that despite a low bulk As concentration in the aquifer matrix, high As concentrations can be generated in groundwater of the Suwannee Limestone in the UFA through the injection of oxygen-rich water, which dissolves As-rich pyrite.

5.3. Role of municipal pumping

Groundwater samples from the two well clusters, DEP-4 and DEP-5 showed much lower As and Mo concentrations than DEP-1, DEP-2 and DEP-3, although they underwent the same water level fluctuations induced by seasonal variations in recharge and pumping from the municipal wells. However, those wells are geographically removed from the center of the study area where As and Mo levels in the DSW were highest. Particularly groundwater samples from the DEP-5 cluster, which is on the other side of the Alafia River (Fig. 1) did not show any As concentrations above 2 µg/L and only one sample had Mo above 40 µg/L. Considering that DEP-5 is closest to the well field (Fig. 5) and undergoes the same water

level fluctuations and drawdown (due to pumping in the well field to the west) as the other four DEP wells it becomes evident neither pumping nor water level fluctuations should be a major cause for the high concentrations in the DSW. Thus, the only obvious difference seems to be the density and abundance of DSW, which were much higher where As and Mo concentrations were high (Fig. 1).

6. Conclusions

While the mobilization of geogenic trace metals is often associated with exogenic pumping-induced hydraulic gradient changes, we find that if the density of multi-aquifer wells is sufficient, the short-circuiting provided by the wells can alter hydrologic flow paths sufficiently to induce the mobilization of geogenic trace metals even in the absence of significant pumping. The short-circuiting of the wells effectively increases the local scale permeability of the aquifer, which results in the mixing of oxygen-rich surface and deeper anoxic ground waters across a confining unit. Because the alterations to the hydrologic flow paths is a consequence of endogenic changes to the physical structure of the aquifer system rather than due to pumping, the changes in flow paths are not easily reversible, thus significantly complicating site remediation. Our results provide a cautionary warning of the risks of undue private domestic well development in rapidly growing communities.

The results from the DEP monitoring wells demonstrate that despite its relatively small area, the geochemical and hydrogeological setting in Lithia is complex and the release of As and Mo into groundwater likely not controlled by a single process. However, in all cases the release of the As and Mo appears to be a consequence of changes in the physiochemical conditions in the aquifer, either via the introduction of oxygen-rich fluids into the UFA or the mixing of different fluids in the IAS.

The current hypothesis for the occurrence of Mo in groundwater in the Lithia area summarizes as follows. Caused by the enhanced permeability provided by the high density of domestic supply wells (DSW) combined with water use from the DSW, seasonal changes and potentially varying pumping rates in the well field to the west, vertical flow directions oscillate and thus cause successions of oxic, anoxic, saturated and under-saturated conditions in the IAS:

1) Movement of oxygenated water from the SAS into the IAS causes the dissolution of pyrite and/or organic matter and As and Mo are released into the groundwater.
2) Should conditions remain oxygenated, HFO can precipitate and scavenge As from the groundwater. At the same time the concentration release of Mo continues until the activity of MoO_4^{2-} is sufficient to cause powellite precipitation i.e., $[MoO_4^{2-}] * [Ca^{2+}] > K_{sp}$.
3) Movement of anoxic water from the UFA into the IAS causes the dissolution of HFO and the release of adsorbed As to the groundwater. Should the conditions remain reducing, then pyrite could precipitate and scavenge As and Mo from groundwater.
4) Mixing of SAS or UFA groundwater with IAS groundwater causes under-saturation within the IAS resulting in the dissolution of powellite.

Acknowledgments

We thank the Florida Department of Environmental Protection Site Investigation Section for making this study possible. Particularly the participation and excellent support by Robert Cilek, Jeff Newton and William Martin was greatly appreciated. Olesya Lazareva, Daniela Stebbins, Angela Dippold, and Bastian Kuehl are thanked for their participation. TP acknowledges partial funding from the German Research Foundation (DFG-Projekt PI 746/1-1). An earlier version of this manuscript benefitted from comments by Kay Hamer and Maria Ruiz-Chancho.

Appendix A. Supplementary data

Supplementary data related to this article can be found at http://dx.doi.org/10.1016/j.apgeochem.2016.03.002.

References

Al Kuisi, M., Al-Hwaiti, M., Mashal, K., Abed, A.M., 2015. Spatial distribution patterns of molybdenum (Mo) concentrations in potable groundwater in northern Jordan. Environ. Monit. Assess. 187.
Alberic, P., Lepiller, M., 1998. Oxydation de la matière organique dans un système hydrologique karstique alimenté par des pertes fluviales (Loiret, France) (Oxidation of organic matter in a karstic hydrologic unit supplied through stream sinks (Loiret, France)). Water Res. 32, 2051–2064.
Amini, M., Abbaspour, K.C., Berg, M., Winkel, L., Hug, S.J., Hoehn, E., Yang, H., Johnson, C.A., 2008. Statistical modeling of global geogenic arsenic contamination in groundwater. Environ. Sci. Technol. 42, 3669–3675.
Amirbahman, A., Sigg, L., Gunten, U.V., 1997. Reductive dissolution of Fe(III) (Hydr) oxides by cysteine: kinetics and mechanism. J. Colloid Interface Sci. 194, 194–206.
Arthur, J.D., Fischler, C., Kromhout, C., Clayton, J., Kelley, G.M., Lee, R.A., Li, L., O'Sullivan, M., Green, R., Werner, C., 2008. Hydrogeologic Framework of the Southwest Florida Water Management District, Florida Geological Survey Bulletin, p. 102.
Ayotte, J.D., Szabo, Z., Facozio, M.J., Eberts, S.M., 2011. Effects of human-induced alteration of groundwater flow on concentrations of naturally-occurring trace elements at water-supply wells. Appl. Geochem. 26, 747–762.
Barcelona, M.J., Helfrich, J.A., 1986. Well construction and purging effects on ground-water samples. Environ. Sci. Technol. 20, 1179–1184.
Bostick, B.C., Fendorf, S., 2003. Arsenite sorption on troilite (FeS) and pyrite (FeS2). Geochim. Cosmochim. Acta 67, 909–921.
Bostick, B.C., Fendorf, S., Helz, G.R., 2003. Differential adsorption of molybdate and tetrathiomolybdate on pyrite (FeS2). Environ. Sci. Technol. 37, 285–291.
Carucci, V., Petitta, M., Aravena, R., 2012. Interaction between shallow and deep aquifers in the Tivoli Plain (Central Italy) enhanced by groundwater extraction: a multi-isotope approach and geochemical modeling. Appl. Geochem. 27, 266–280.
Conlan, M.J.W., Mayer, K.U., Blaskovich, R., Beckie, R.D., 2012. Solubility controls for molybdenum in neutral rock drainage. Geochem. Explor. Environ. Anal. 12, 21–32.
Delemos, J.L., Bostick, B.C., Renshaw, C.E., Stürup, S., Feng, X., 2006. Landfill-stimulated iron reduction and arsenic release at the Coakley superfund site (NH). Environ. Sci. Technol. 40, 67–73.
Deverel, S.J., Millard, S.P., 1988. Distribution and mobility of selenium and other trace-elements in shallow groundwater of the western San Joaquin Valley, California. Environ. Sci. Technol. 22, 697–702.
Essington, M.E., 1992. Formation of calcium and magnesium molybdate complexes in dilute aqueous solutions. Soil Sci. Soc. Am. J. 56, 1124–1127.
Felmy, A., Rai, D., Mason, M., 1992. The solubility of CaMoO4(c) and an aqueous thermodynamic model for Ca2+-MoO 4 2 -ion-interactions. J. Solut. Chem. 21, 525–532.
Ferguson, J.F., Gavis, J., 1972. A review of the arsenic cycle in natural waters. Water Res. 6, 1259–1274. Pergamon Press.
Food and Nutrition Board, I.o.M., 2001. Molybdenum, Dietary Reference Intakes for Vitamin a, Vitamin K, Boron, Chromium, Copper, Iron, Manganese, Molybdenum, Nickel, Silicon, Vanadium, and Zinc. National Academy Press, Washington, D.C., pp. 420–441
Freeze, R.A., Witherspoon, P.A., 1966. Theoretical analysis of regional groundwater flow: 1. Analytical and numerical solutions to the mathematical model. Water Resour. Res. 2 (4), 641–656.
Green, R., Arthur, J.D., DeWitt, D., 1995. Lithostratigraphic and Hydrostratigraphic Cross Sections through Pinellas and Hillsborough Counties, Southwest Florida. United States Geological Survey Open File Report, p. 26.
Harbaugh, A.W., 2005. MODFLOW-2005, the U.S. Geological Survey Modular Ground-water Model – the Ground-water Flow Process. U.S. Geol. Surv. Techniques and Methods 6–A16.
Harvey, C.F., Ashfaque, K.N., Yu, W., Badruzzaman, A.B.M., Ali, M.A., Oates, P.M., Michael, H.A., Neumann, R.B., Beckie, R., Islam, S., Ahmed, M.F., 2006. Groundwater dynamics and arsenic contamination in Bangladesh. Chem. Geol. 228, 112–136.
Harvey, C.F., Swartz, C.H., Badruzzaman, A.B.M., Keon-Blute, N., Yu, W., Ali, M.A., Jay, J., Beckie, R., Niedan, V., Brabander, D., Oates, P.M., Ashfaque, K.N., Islam, S., Hemond, H.F., Ahmed, M.F., 2002. Arsenic mobility and groundwater extraction in Bangladesh. Science 298, 1602–1606.
Hughes, J.D., Vacher, H.L., Sanford, W.E., 2009. Temporal response of hydraulic head,

temperature, and chloride concentrations to sea-level changes, Floridan aquifer system, Usa. Hyrogeol. J. 17, 793–815.
Jambor, J.L., Dutrizac, J.E., 1998. Occurrence and constitution of natural and synthetic ferrihydrite, a widespread iron oxyhydroxide. Chem. Rev. 98, 2549–2585.
Johannesson, K.H., Lyons, W.B., Graham, E.Y., Welch, K.A., 2000. Oxyanion concentrations in eastern Sierra Nevada rivers – 3. Boron, molybdenum, vanadium, and tungsten. Aquat. Geochem. 6, 19–46.
Jones, G.W., Pichler, T., 2007. The relationship between pyrite stability and arsenic mobility during aquifer storage and recovery in southwest central Florida. Environ. Sci. Technol. 41, 723–730.
Katz, B.G., Crandall, C.A., Metz, P.A., McBride, W.S., Berndt, M.P., 2007. Chemical Characteristics, Water Sources and Pathways, and Age Distribution of Ground Water in the Contributing Recharge Area of a Public-supply Well Near Tampa, Florida, 2002-05. USGS Scientific Investigations Report 2007-5139, p. 85.
Katz, B.G., McBride, W.S., Hunt, A.G., Crandall, C.A., Metz, P.A., Eberts, S.M., Berndt, M.P., 2009. Vulnerability of a public supply well in a karstic aquifer to contamination. Ground Water 47, 438–452.
Kendall, C., Coplen, T.B., 2001. Distribution of oxygen-18 and deuterium in river waters across the United States. Hydrol. Process. 15, 1363–1393.
Korte, N.E., Fernando, Q., 1991. A review of arsenic (III) in groundwater. Crit. Rev. Environ. Control 21, 1–36.
Koterba, M.T., Wilde, F.D., Lapham, W.W., 1995. Groundwater Data Collection Protocols and Procedures for the National Water Quality Assessment Program: Collection and Documentation of Water-quality Samples and Related Data. US Geol. Surv. Open-File Report 95–399.
Lazareva, O., Druschel, G., Pichler, T., 2015. Understanding arsenic behavior in carbonate aquifers: implications for aquifer storage and recovery (ASR). Appl. Geochem. 52, 57–66.
Lazareva, O., Pichler, T., 2007. Naturally occurring arsenic in the miocene hawthorn group, southwestern Florida: implication for phosphate mining. Appl. Geochem. 22, 953–973.
Leybourne, M.I., Cameron, E.M., 2008. Source, transport, and fate of rhenium, selenium, molybdenum, arsenic, and copper in groundwater associated with porphyry-Cu deposits, Atacama Desert, Chile. Chem. Geol. 247, 208–228.
McNeill, L.S., Hsiao-wen, C., Edwards, M., 2002. Aspects of arsenic chemistry in relation to occurrence, health and treatment. In: Frankenberger Jr., W.T. (Ed.), Environmental Chemistry of Arsenic. Marcel Dekker, New York, pp. 141–154.
Miller, J.A., 1986. Hydrogeologic Framework of the Floridan Aquifer System in Florida, Georgia, South Carolina and Alabama.
Nicolli, H.B., Suriano, J.M., Peral, M.A.G., Ferpozzi, L.H., Baleani, O.A., 1989. Groundwater contamination with arsenic and other trace-elements in an area of the Pampa, province of Cordoba, Argentina. Environ. Geol. Water Sci. 14, 3–16.
Peters, S.C., Blum, J.D., 2003. The source and transport of arsenic in a bedrock aquifer, New Hampshire, Usa. Appl. Geochem. 18, 1773–1787.
Pichler, T., 2005. δ34S isotope values of dissolved sulfate (SO42-) as a tracer for battery acid (H2SO4) contamination. Environ. Geol. 47, 215–224.
Pichler, T., Mozaffari, A., 2015. Occurrence, distribution and mobility of geogenic molybdenum and arsenic in a limestone aquifer matrix. Appl. Geochem. 63, 623–633.
Pichler, T., Price, R.E., Lazareva, O., Dippold, A., 2011. Determination of arsenic concentration and distribution in the Floridan aquifer system. J. Geochem. Explor. 111, 84–96.
Pichler, T., Sültenfuß, J., 2010. A stable and radioactive isotope study of geogenic arsenic contamination in a limestone aquifer. In: Levin, C., Grathwohl, P., Kappler, A., Kaufmann-Knoke, R., Rügner, H. (Eds.), Grundwasser für die Zukunft. E. Schweizerbart, Tübingen, p. 62.
Pichler, T., Veizer, J., Hall, G.E.M., 1999. Natural input of arsenic into a coral-reef ecosystem by hydrothermal fluids and its removal by Fe(III) oxyhydroxides. Environ. Sci. Technol. 33, 1373–1378.
Plummer, L.N., Rupert, M.G., Busenberg, E., Schlosser, P., 2000. Age of irrigation water in ground water from the eastern snake river plain aquifer, south-central Idaho. Ground Water 38, 264–283.
Price, R.E., Pichler, T., 2006. Abundance and mineralogical association of arsenic in the Suwannee limestone (Florida): implications for arsenic release during water–rock interaction. Chem. Geol. 228, 44–56.
Sacks, L.A., Tihansky, A.B., 1996. Geochemical and Isotopic Composition of Ground Water with Emphasis on Sources of Sulfate in the Upper Floridan Aquifer and Intermediate Aquifer System in Southwest Florida. U.S. Geological Survey, Tallahassee, p. 70.
Scott, T.M., 1988. Lithostratigraphy of the Hawthorn Group (Miocene) of Florida. Florida Geological Survey Bulletin, pp. 1–148.
Scott, T.M., 1990. The Lithostratigraphy of the Hawthorn Group of Peninsular Florida. Florida Geologica Survey Open File Report 36, Open file report. FGS.
Solomon, D.K., Cook, P.G., 2000. 3H and 3He. In: Cook, P.G., Herczeg, A.L. (Eds.), Environmental Tracers in Subsurface Hydrology. Kluwer Academic Publishers, Boston, Mass, pp. 397–424.
Solomon, D.K., Poreda, R.J., Schiff, S.L., Cherry, J.A., 1992. Tritium and helium 3 as groundwater age tracers in the Borden Aquifer. Water Resour. Res. 28, 741–755.
Stewart, J.W., Goetz, C.L., Mills, L.R., 1978. Hydrogeologic Factors Affecting the Availability and Quality of Ground Water in the Temple Terrace Area, Hillsborough County, Florida. US Geol. Surv. Water-Resources Investigations 78–4.
Sultenfuß, J., Rhein, M., Roether, W., 2009. The Bremen mass spectrometric facility for the measurement of helium isotopes, neon, and tritium in water. Isot. Environ. Health Stud. 45, 1–13.
Thornthwaite, C.W., 1948. An approach toward a rational classification of climate. Geogr. Rev. 38, 55–94.
Tribovillard, N., Riboulleau, A., Lyons, T., Baudin, F., 2004. Enhanced trapping of molybdenum by sulfurized marine organic matter of marine origin in mesozoic limestones and shales. Chem. Geol. 213, 385–401.
Wallis, I., Prommer, H., Pichler, T., Post, V., Norton, S.B., Annable, M.D., Simmons, C.T., 2011. Process-based reactive transport model to quantify arsenic mobility during aquifer storage and recovery of potable water. Environ. Sci. Technol. 45, 6924–6931.
Welch, A.H., Lico, M.S., 1998. Factors controlling As and U in shallow ground water, southern Carson Desert, Nevada. Appl. Geochem. 13, 521–539.